

# A Segmental Polynomial Model of Ventricular Electrograms as a Simple and Efficient Morphology Discriminator for Implantable Devices

Jeffrey L. Williams, M.D., M.S., Vladimir Shusterman, M.D., Ph.D.,  
and Samir Saba, M.D.

*From the University of Pittsburgh, Pittsburgh, PA*

**Background:** The goal of this study is to construct a polynomial model of the ventricular electrogram (EGM) that faithfully reproduces the EGM and can be implemented in current, low computational power implantable devices. Such a model of ventricular EGMs is still lacking.

**Methods:** New Zealand White rabbits underwent chronic implantation of pacemakers through a left thoracotomy approach. Unipolar ventricular EGMs sampled at a frequency of 1 kHz were stored digitally in 1-minute segments before and after intravenous injection of isoproterenol or procainamide. Each cardiac cycle was divided into a QR and an RQ segment which were modeled separately using a 6th order polynomial equation.

**Results:** The 14 coefficients of each cardiac cycle were reproducible throughout the baseline recordings ( $r \geq 0.94$ ,  $P < 0.002$ ). Isoproterenol caused no changes in the coefficients of the QR segment but significantly altered all but one of the seven coefficients of the RQ segment ( $p_6 = 0.0039$ ,  $p_5 = 0.017$ ,  $p_4 = 0.00007$ ,  $p_3 = 0.112$ ,  $p_2 = 0.00016$ ,  $p_1 = 0.0086$ ,  $p_a = 0.00003$ ). Procainamide caused statistically significant changes in both QR segment ( $p_6 = 0.018$ ,  $p_5 = 0.287$ ,  $p_4 = 0.019$ ,  $p_3 = 0.176$ ,  $p_2 = 0.016$ ,  $p_1 = 0.362$ ,  $p_a = 0.000044$ ) and RQ segment ( $p_6 = 0.0028$ ,  $p_5 = 0.036$ ,  $p_4 = 0.002$ ,  $p_3 = 0.058$ ,  $p_2 = 0.022$ ,  $p_1 = 0.718$ ,  $p_a = 0.0018$ ) coefficients.

**Conclusion:** Our data demonstrate the feasibility of a segmental polynomial equation that reproduces the phases of depolarization and repolarization of the rabbit EGM. This model is reproducible and demonstrates the expected changes with antiarrhythmic drug administration. If reproduced in humans, these findings can have wide applications in patients with implantable devices, ranging from morphologic discrimination of arrhythmias to early detection of metabolic derangements or drug effects.

**A.N.E. 2006;11(3):271-280**

electrogram; polynomial; model; rabbit

## BACKGROUND

The morphology of the ventricular electrogram (EGM) reflects local and global electrical activity of the heart. There has been a dramatic increase in the utilization of implantable cardioverter defibrillators and as a result, there is an abundance of EGM information available. However, few attempts have been made to extract information from the EGMs aside from the discrimination of supraventricular (SVT) and ventricular tachycardias (VT).

The current study aims to construct a mathematical model of sufficient power to faithfully reproduce the raw electrical signal of the rabbit ventric-

ular EGM while preserving computational simplicity to permit implementation in current, low computational power implantable devices. This study will assess the reproducibility and response of the model to pharmacologic interventions with known cardiac effects.

## METHODS

### Pacemaker Implantation

New Zealand White rabbits ( $n = 8$ ) weighing 4–5 kg underwent chronic implantation of a single-chamber pacemaker (Medtronic Inc., Minneapolis,

---

*Address for reprints: Samir Saba, M.D., Division of Cardiac Electrophysiology, University of Pittsburgh Medical Center, PUH B535, 200 Lothrop Street, Pittsburgh, PA 15213. Fax: (412) 647-7979; E-mail: williamsjl4@upmc.edu*

MN, USA ) in a protocol approved by the University of Pittsburgh Institutional Animal Care and Use Committee. Each rabbit was induced with Ketamine and Xylazine (40 mg/kg and 5 mg/kg) intramuscularly. A 20G catheter was placed in the ear vein for fluids (37 degree, 5% dextrose) administration. A 20G arterial line was placed in the rabbit ear for continuous hemodynamic monitoring. The rabbit was then intubated (size 2–3 endotracheal tube), ventilated, and maintained on Isoflurane (2.0–2.5%). The animals then underwent placement of a single right ventricular pacing lead through a left-sided thoracotomy. The lead was connected to a single chamber pacemaker (Kappa 400, Medtronic, Saint Paul, MN, USA) programmed to deliver backup pacing at a rate no lower than 100 beats/min. The pacemaker lead was tunneled to the abdomen where the pacemaker pocket was created. The pacemaker pocket was closed with a 2.0 and 5.0 polysorb suture material in three separate layers. The pacemakers were used to obtain unipolar EGMs (from RV tip to pacemaker can) over a period of weeks without having to utilize percutaneous leads. The animals were anesthetized for the entire procedure, which was completed under aseptic conditions. After surgery, the animals were placed on a circulating water heating pad until recovery. They received antibiotics and analgesia. Rabbits were allowed to recover from surgery for 1 week prior to further study.

### Data Acquisition

On the day of data acquisition, the rabbits were anesthetized using ketamine and xylazine and ventricular EGMs were obtained before receiving either isoproterenol or procainamide. Rabbits were given one dose of isoproterenol 5 mcg/kg and after 5 minutes, 1 minute of EGMs were recorded. After 30 minutes elapsed since initial dose, the same rabbit was given isoproterenol 10 mcg/kg intravenously. Again, 1 minute of EGMs was recorded 5 minutes after the injection. Rabbits were also given one dose of procainamide 5 mg/kg intravenously and after 5 minutes, 1 minute of EGMs were recorded. After 30 minutes elapsed since initial dose, this same rabbit was given procainamide 15 mg/kg intravenously. Again, 1 minute of EGMs were recorded 5 minutes after the injection. Each rabbit was given only one type of medication on a study day and at least 3 days elapsed before a new medication was introduced. The pacemaker EGMs

were recorded in real-time using a custom data acquisition system.

The data acquisition system was based on a Pentium M laptop PC (Hewlett-Packard, Palo Alto, CA, USA) with a PCMCIA-based 200 kS/s, 16-bit, 16-channel, multifunction analog-to-digital converter (ADC) (NI DAQCard-6036E, National Instruments, Austin, TX, USA). The raw EGMs were input to a two-channel isolated, analog input (SCCAI07, National Instruments) contained in a shielded carrier (SC2345, National Instruments) cabled to the ADC. The SCC modules are installation rated for Category II, and provide safety working isolation of 300 V per module. The raw EGMs were then saved to the laptop's harddrive using VI-Logger Software (National Instruments, Austin).

### Data Analysis and Statistics

The raw data were processed using Matlab (MathWorks, Natick, MA, USA). All unipolar EGMs from each rabbit were standardized to that rabbit's baseline EGM mean and standard deviation. This centering and scaling transformation improves the numerical properties of both the polynomial and the fitting algorithm. They were then

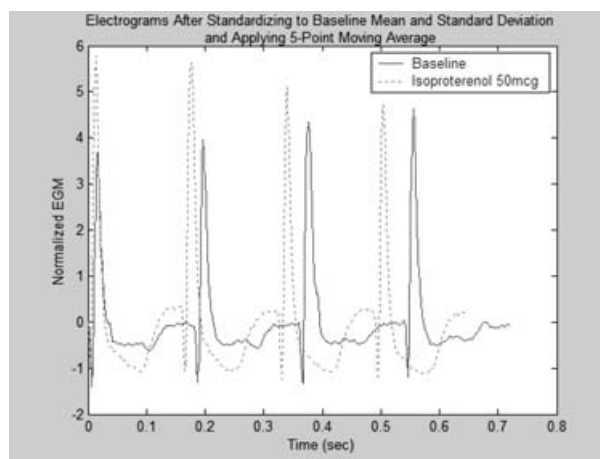


**Figure 1.** Electrograms after standardizing to the baseline EGM's mean and standard deviation and applying a 5-point moving average. Four consecutive EGMs were taken from the 60 second recording at baseline and after medication administration. These EGMs were then standardized to that rabbit's baseline EGM mean and standard deviation and subject to a 5-point moving average. The baseline EGM is shown with solid line and the EGM after 10 mcg/kg (50 mcg) isoproterenol is shown with dotted line.

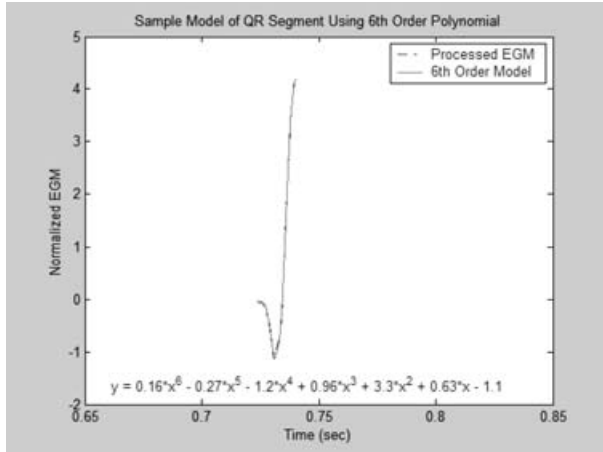


**Figure 2.** Sample EGM QR segment fit to a 6th order polynomial. The raw EGM was processed as described in the Methods. A 6th order polynomial was then fitted to this QR segment. The equation shown in this figure depicts the coefficients that were then used for subsequent analysis.

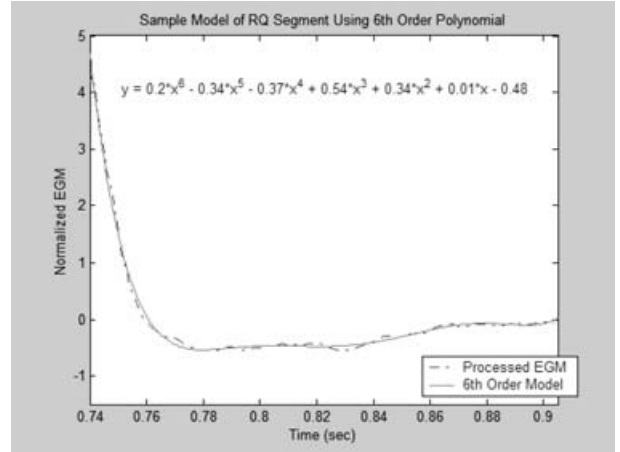


**Figure 3.** Sample EGM RQ segment fit to a 6th order polynomial. The raw EGM was processed as described in the Methods. A 6th order polynomial was then fitted to this RQ segment. The equation shown in this figure depicts the coefficients that were then used for subsequent analysis.

subjected to a 5-point moving average as shown in Figure 1.

The peak of the R wave is the most visually and computationally identifiable component of the EGM. Thus, the identification of this point was chosen as the first step in the signal analysis. Next, the EGM was divided into two “segments,” the QR and RQ. This segmentation simplifies signal analysis while preserving all the attributes of the original signal. The earliest deflection of the QRS was taken as the onset of the initial segment (QR segment). The initial segment is denoted QR though not all EGMs will contain a Q wave. The peak of the R wave was taken as the end of the QR segment.

The second segment, RQ, spans from the peak of the R wave to the earliest onset of the subsequent EGM. Thus, the combination of the RQ and QR segments preserves all features of depolarization and repolarization of the original EGM.

Using Matlab, each segment of the processed EGM was then fit to a 6th order polynomial equation using the *polyfit* function ( $a = \text{polyfit}(x,y,n)$ ). This function assigns coefficients to the modeled polynomial  $a(x)$  of degree  $n$  to fit the EGM while minimizing error with a least-squares algorithm. The resulting  $a(x)$  is a row vector of length  $n + 1$  containing the polynomial coefficients in descending powers:

$$a(x) = a_1x^n + a_2x^{n-1} + L + a_nx + a_{n+1}$$

Examples of the specific functions (with the corresponding coefficients) used for modeling the EGM are depicted in Figures 2 and 3. The order of the polynomial used to model the segmented EGM was determined by fitting polynomials of increasing order and selecting the model that maximized modeling accuracy while limiting computational complexity. Residuals are the differences between the observed values and the fitted values. In Matlab, both the observed values and modeled values are stored in matrices. The norm of the matrix of residuals is a scalar that attempts to quantify the magnitude of the residuals in that matrix. In general, a smaller norm indicates a better model fit. The higher the degree of polynomial chosen the lower the resulting norms of residuals and hence, better model fit. In an attempt to balance model order with computational complexity, we analyzed the norms of residuals for typical baseline EGM QR and RQ segments to determine the incremental benefit as higher order polynomials were used. We empirically limited our model order to the point at which there ceased to be a greater than 20% decrease in the norm of residuals as we increased the model order by one starting with a linear regression. For the baseline QR and RQ segments analyzed, the 6th order polynomial was found to be the model at which further increases in order resulted in less than 20% decreases in the norms of

residuals. Thus, we were able to maximize modeling accuracy while limiting computational complexity. Figure 2 depicts a sample EGM QR segment fit to a 6th order polynomial. Figure 3 depicts a sample EGM RQ segment fit to a 6th order polynomial.

To assess correlation and reproducibility during the baseline 1-minute EGM recordings, four consecutive EGMs were taken at  $t = 0$  second,  $t = 25$  second, and  $t = 50$  second. Next, the coefficients of the polynomial model were determined for each set (at each of the three time points) of four QR and RQ segments. The means of the QR and RQ coefficients of EGMs at  $t = 0$  second,  $t = 25$  second, and  $t = 50$  second were first compared using a paired samples *t*-Test on SPSS software V10.1.0 (SPSS Inc., Chicago, IL, USA) to assess for baseline correlation of the model coefficients over the recording period. Then, using the methods described by Bland and Altman,<sup>1</sup> the reproducibility of these coefficients was then evaluated using a one-way analysis of variance for four correlated samples at times  $t = 0$  second,  $t = 25$  second, and  $t = 50$  second. For this analysis, the null hypothesis ( $H_0$ ) assumes that there is no difference between measured coefficients at the various times over the baseline recording period.

Subsequently, four consecutive EGMs were analyzed at baseline and after medication administration. The coefficients of the polynomial model were determined for the QR and RQ segments of each of the four cycles. Statistical comparisons between the coefficients (mean  $\pm$  standard deviation) of the segmental, polynomial model during baseline and with each medication were performed using a 2-tailed, paired Student's *t*-test on SPSS software. A  $P$  value  $\leq 0.05$  was considered statistically significant. We then performed a quantitative analysis of the model errors on the baseline EGMs and after both isoproterenol and procainamide.

## RESULTS

### Correlation and Reproducibility of the Model

Four consecutive EGMs were taken at  $t = 0$ ,  $t = 25$  second, and  $t = 50$  second during the baseline 60 second EGM recordings. Next, the coefficients of the polynomial model were determined for the QR and RQ segments of each of the 12 cycles. The means of the QR and RQ coefficients for each set

of four consecutive EGM's at  $t = 0$ ,  $t = 25$ , and  $t = 50$  second were then compared using a 2-tailed, paired samples *t*-test. The seven coefficients representing the QR segment exhibited a high level of correlation at times  $t = 0$  second,  $t = 25$  second, and  $t = 50$  second ( $R = 0.962$ ,  $P = 0.001$ , for  $t = 0$  second and  $t = 25$  second,  $R = 0.939$ ,  $P = 0.002$ , for  $t = 0$  second and  $t = 50$  second, and  $R = 0.997$ ,  $P = 0.001$ , for  $t = 25$  second and 50 second). The seven coefficients representing the RQ segment exhibited a high level of correlation at times  $t = 0$  second,  $t = 25$  second, and  $t = 50$  second ( $R = 0.993$ ,  $P = 0.001$ , for  $t = 0$  second and  $t = 25$  second,  $R = 0.999$ ,  $P = 0.002$ , for  $t = 0$  second and  $t = 50$  second, and  $R = 0.994$ ,  $P = 0.001$ , for  $t = 25$  second and 50 second).

As noted above, four consecutive EGMs were taken at  $t = 0$ ,  $t = 25$  second, and  $t = 50$  second during the baseline 60 second EGM recordings. Next, the coefficients of the polynomial model were determined for the QR and RQ segments of each of the 12 cycles. Then, using the methods described by Bland and Altman,<sup>1</sup> the reproducibility of these coefficients was then evaluated using a one-way analysis of variance for four correlated samples at times  $t = 0$  second,  $t = 25$  second, and  $t = 50$  second. After we applied the one-way analysis of variance with these repeated measurements, we obtained  $P$  values  $> 0.05$ . Thus, we concluded there was no difference between measured coefficients at the various times over the baseline 60 second recording period.

### Changes in Model Coefficients with Isoproterenol

There were no statistically significant changes in the coefficients of the QR model when baseline is compared to the 10 mcg/kg (50 mcg) dose of isoproterenol. The average norm of residuals for the 6th order polynomial model of the four QR segments at baseline and after 10 mcg/kg of isoproterenol were 0.373 and 0.565, respectively. Figure 4 depicts the coefficients of the 6th order polynomial model of RQ segment changes from baseline to 10 mcg/kg of isoproterenol. There were statistically significant changes ( $P \leq 0.05$ ) in the constant, 1st, 2nd, 4th, 5th, and 6th order coefficients of the RQ model when baseline is compared to the 10 mcg/kg (50 mcg) dose of isoproterenol. The average norm of residuals for the 6th order polynomial model of the four RQ segments at

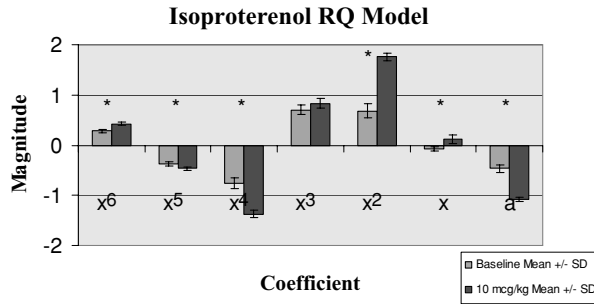


**Figure 4.** Coefficients of 6th order polynomial model of RQ segment changes from baseline to 10 mcg/kg of isoproterenol. Four consecutive EGMs were analyzed at baseline and after medication administration. The coefficients of the polynomial model were then determined for the RQ segments of each of the four cycles and depicted as a mean and standard deviation in this figure. There were statistically significant changes ( $P \leq 0.05$ , denoted by \* in the Figure) in the constant, 1st, 2nd, 4th, 5th, and 6th order coefficients of the RQ model when baseline is compared to the 10 mcg/kg dose of isoproterenol.

baseline and after 10 mcg/kg of isoproterenol were 0.994 and 1.015, respectively.

### Changes in Model Coefficients with Procainamide

Figure 5 depicts the coefficients of the 6th order polynomial model of QR segment changes from baseline to 15 mg/kg of procainamide. There were statistically significant changes in the constant,

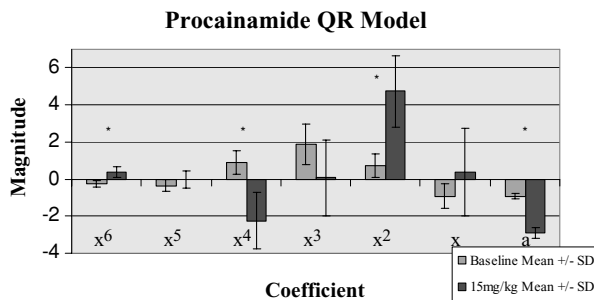


**Figure 5.** Coefficients of the 6th order polynomial model of QR segment changes from baseline to 15 mg/kg of procainamide. Four consecutive EGMs were analyzed at baseline and after medication administration. The coefficients of the polynomial model were then determined for the QR segments of each of the four cycles and depicted as a mean and standard deviation in this figure. There were statistically significant changes ( $P \leq 0.05$ , denoted by \* in the figure) in the constant, 2nd, 4th, and 6th order coefficients of the QR model when baseline is compared to the 15 mg/kg dose of procainamide.

2nd, 4th, and 6th order coefficients of the QR model when baseline is compared to the 15 mg/kg dose of procainamide. The average norm of residuals for the 6th order polynomial model of the four QR segments at baseline and after 15 mg/kg of procainamide were 0.829 and 0.955, respectively. There were statistically significant changes in the constant, 2nd, 4th, 5th, and 6th order coefficients of the RQ model when baseline is compared to the 15 mg/kg dose of procainamide. The average norm of residuals for the 6th order polynomial model of the four RQ segments at baseline and after 15 mg/kg of procainamide were 4.965 and 1.2, respectively.

## DISCUSSION

This study demonstrated that a segmental polynomial model can reproduce phases of depolarization and repolarization of the rabbit ventricular EGM while preserving all the attributes of the entire EGM at baseline and under the effect of select antiarrhythmic medications. This model's simplicity permits implementation into current implantable devices that have limited computing power, while at the same time, may potentially provide insight into phases of the cardiac action potential (AP). The waveform analysis process allows the EGMs to be modeled with a total of 14 coefficients that are then evaluated for significant changes in magnitude with both isoproterenol and procainamide. We derived our model's segmental structure and order based upon preliminary animal studies and then quantified the medications that resulted in primarily QR changes (procainamide) and RQ changes (isoproterenol), thus validating its ability to detect changes induced by known pharmacological interventions. The rabbit was chosen as the animal model for this study because it is the smallest animal that can accommodate size-wise the implantation of pacing leads on the heart. Also, it is the smallest animal model that is very similar to humans from the electrophysiologic standpoint (e.g., cardiac ion channels), which renders the extrapolation of the results of this study relatively straightforward.

Isoproterenol has no known sodium channel effects therefore, as expected there were no statistically significant changes in the coefficients of the QR segment model. However, the data demonstrated that isoproterenol caused predominantly T wave changes that resulted in statistically significant changes in all but one of the RQ segment

model coefficients. Accurately capturing changes in the RQ segment leads us to believe that this model may have utility in detecting phenomena such as ischemia or electrolyte disturbances, which are known to cause ST segment and T wave alterations. The unipolar, as opposed to bipolar, EGM facilitates the model's ability to detect far-field electrical activity such as ischemia.

Procainamide caused statistically significant changes in both QR segment and RQ segment models. Procainamide is primarily a sodium channel blocker that can cause depolarization changes due to its effects on Phase 0 of the cardiac AP. In addition, procainamide is also a potassium channel blocker. Segment QR represents a summation of Phases 0 and 1 of the cardiac AP<sup>2-4</sup> and may give insight into maximal upstroke velocity (Vmax) and AP amplitude.<sup>5,2</sup> Quantifying changes in both of the QR and RQ segments may provide a useful tool in assessing the effects of existing and new antiarrhythmic drugs on Phases 0-1 of the cardiac AP and on ventricular repolarization.

### Electrogram Modeling

Mathematical modeling of the surface electrocardiogram (ECG) has been shown to be feasible using various methods.<sup>6,7</sup> Parametric<sup>6</sup> and autoregressive<sup>7</sup> modeling are two techniques that have been used to faithfully reproduce the surface ECG, albeit at the expense of using a large number of coefficients. For example, while Mukhopadhyay et al.<sup>6</sup> utilized a total of 28 coefficients to develop their parametric model, Dingfei et al.<sup>7</sup> used autoregressive modeling to characterize cardiac arrhythmias with four coefficients at each point over a full cardiac cycle, thus utilizing a total number of coefficients equal to four times the sampling frequency.

Attempts at modeling the cardiac epicardial and endocardial EGMs have been scarce. Correlation waveform analysis has been used to capture the morphology of ventricular EGM during cardiac arrhythmia and to compare it to the same EGM during normal rhythm.<sup>8-10</sup> These correlation techniques reflect overall morphologic similarity between EGM beats, however they do not "model" the EGM per se. Correlation techniques are not affected by heart rate increases, though an increase in amplitude is often seen with increasing sympathetic tone.<sup>11</sup> There are numerous other techniques attempting to discriminate between arrhythmias based on changes in ventricular EGM morphology.

One such technique based the morphology analysis on the first derivative of the EGM which was then compared to templates obtained during sinus rhythm.<sup>12-14</sup> Unpublished data from our laboratory demonstrate that wavelet decomposition can reproduce the ventricular EGM quite accurately, albeit with a number of coefficients exceeding 50. Orthogonal expansions such as singular-value decomposition and Karhunen-Loeve transform (principal-component analysis) are known to be optimal mathematical solutions to EGM analysis<sup>15-18</sup> however, this is at a cost of considerable additional computational complexity.<sup>19</sup> In addition, there is controversy surrounding the applicability of ascribing any physiologic significance to the data resulting from such decompositions.<sup>20</sup> The polynomial model proposed here (ultimately intended for use in implantable devices) is computationally simple and for this application, computational efficiency outweighs mathematical optimization.

### Electrogram Model to Assess Underlying Cardiac Ion Channel Function

The EGM reflects the electrical properties of the myocardium and prior research suggests that it also represents the underlying substrate. The AP of individual cardiac cells has been modeled using a modified FitzHugh-Nagumo reaction-diffusion state equations system.<sup>21</sup> A three dimensional lattice of these modeled cells, incorporating variables of excitability, refractoriness, and ischemia, was used to generate an EGM. Finally, there has been very interesting work studying the effects of antiarrhythmic drugs on epicardial activation of isolated rabbit hearts using a 256 electrode system.<sup>22</sup> These studies have demonstrated pronounced disturbance of the ventricular electrical activation with the use of antiarrhythmic agents. Thus, these studies suggest that the EGM may be used to assess changes in the underlying myocardial substrate. The literature lacks however a simple model for the in vivo assessment and quantification of cardiac APs via ventricular EGM signals.

The ability to quantify changes in the ventricular EGM using this polynomial representation might be used to gain insight into both electrical and structural properties of the underlying myocardium in other physiologic situations. A wide variety of experimental work has shown that the EGM contains information regarding: (1) The myocardial AP and junctional resistance;<sup>23</sup> (2) Changes in the maximal

rise of the AP;<sup>24</sup> (3) Changes in AP amplitude and propagation velocity;<sup>25</sup> (4) Fragmented epicardial activities which may predispose to ventricular tachycardia;<sup>26</sup> (5) Biodomain conductivities and myocardial fiber architecture;<sup>27</sup> (6) Frequency differences between sinus rhythm and VT;<sup>28</sup> and (7) The direction of excitation.<sup>29–32</sup>

The potential utility of this model lies in its ability to capture the phenomena occurring during Phases 0 and 1 of the AP but also during repolarization (Phases 2–4 of the cardiac AP). As discussed above, there is much evidence suggesting that the EGM contains far more information about both the electrical, structural, and chemical properties of the myocardium than commonly thought. The generation of the ventricular cardiac AP is dependent upon the underlying transmembrane ion currents. Phase 0, the upstroke of the AP, represents depolarization of the membrane and is mostly derived from the fast inward sodium current ( $I_{Na}$ ). The peak slope of this upstroke represents the  $V_{max}$ .<sup>5</sup> Phase 1 (initial repolarization) is due to the transient outward current,  $I_{to}$ , which increases in density from endocardium to epicardium.<sup>33</sup> Phase 2 (plateau phase) is primarily due to the delayed rectifier currents  $I_{Kr}$  and  $I_{Ks}$ . The AP amplitude is defined as the voltage from the baseline resting voltage to the crest of the plateau phase (not the peak of the upstroke).<sup>2</sup> The delayed rectifier currents are the major repolarization currents in larger mammals.<sup>34</sup> Phase 3 (late repolarization) is due to the strong inward rectifier current,  $I_{K1}$ , and to a lesser extent,  $I_{Kr}$  and  $I_{Ks}$ . Phase 4 (resting phase) is primarily due to the strong inward rectifier current,  $I_{K1}$ .

In developing an algorithm to analyze EGMs from ICD's, it is useful to understand the electrophysiologic changes associated with ischemia that may predispose a patient to ventricular arrhythmias. Ischemia causes changes to Phases 0 and 1 of the cardiac AP. These changes include depolarization of the resting membrane followed by a decrease in AP amplitude and upstroke velocity.<sup>35,5</sup> Whalley et al.,<sup>5</sup> found that ischemia caused a 32% reduction in AP amplitude ( $P < 0.001$ ) and 66% reduction in  $V_{max}$  ( $P < 0.001$ ). In addition, an elevation of extracellular potassium concentration during ischemia also contributes to the decrease in  $V_{max}$ .<sup>5</sup> Similarly, ischemia has known effects Phases 2–4 of the cardiac AP which can be demonstrated via analysis of repolarization on the EGM. The monophasic AP has a much lower amplitude than the intracellular AP however, the monophasic

AP's can still detect the intracellular AP changes associated with ischemia.<sup>36,37</sup> Finally, the subendocardium plays a pivotal role in most ventricular arrhythmias.<sup>35,38–40</sup>

We have proposed a method of segmenting the EGM that serves as an initial step in analyzing cardiac EGMs available from ICD's in terms of phases of the cardiac AP. This method may allow insight into the Phase 0–1 of the cardiac AP while preserving all the attributes of the entire EGM. The heart depolarizes from endocardium to epicardium and, in a general sense, from apex to base.<sup>2</sup> The earliest deflection of the QRS corresponds to the onset of Phase 0 in the endocardial monophasic action potential (MAP).<sup>2,41</sup> The earliest deflection of the QRS was taken as the onset of the initial segment (Segment QR) in this proposed model. The peak of Phase 0 of the epicardial base MAP, at least in the murine heart, correlated with the return to baseline of the initial and usually dominant waveform of the QRS.<sup>2</sup> In addition, it has been recently demonstrated in canine ventricular wedge preparations that the peak of the major deflection of the QRS complex occurs before the peak of Phase 0 in the epicardial AP.<sup>3</sup> Finally, Aslanidi et al.<sup>4</sup> developed a model of transmural AP propagation in a one dimensional virtual ventricular wall. They demonstrated that the summation of Phases 0–1 of endocardial and M-cell APs forms the segment from the earliest onset of the QRS to the peak of the R wave. Thus, the peak of the R wave was taken as the end of this first segment, QR. Segment QR represents a summation of Phases 0 and 1 of the endocardial AP (and M-cell AP) and may give insight into  $V_{max}$  and AP amplitude. Of course, Segment QR represents a summation of Phases 0 and 1 of multiple cells and regions of the subendocardium and mid-myocardium of the heart at the same time, thus this potential may differ from single cell recordings under conditions of extreme local dispersion of activation and repolarization.<sup>37</sup> Segment QR would contain elements of  $I_{to}$  for both endocardial and M cells however, these channels have the highest concentration in the epicardium.<sup>33,4</sup> Thus, the effects of  $I_{to}$  are most pronounced in the epicardium and thus excluded from the QR segment.

The second segment, RQ, spans from the peak of the R wave to the earliest onset of the subsequent EGM. This would then represent a summation of the remaining Phases of the cardiac cycle which includes the entire T wave. In the case of ischemia, one must be careful to consider that the

unipolar EGM is very dependent upon the relation between the region of ischemia and the vector of the far-field EGM recorded. This segmental model of the cardiac EGM serves as a first step in analyzing waveforms available from ICD's in terms of AP phases and hence, underlying cardiac channel activity.

### Implementation of the Model in Current Generation of ICDs

The polynomial model of the rabbit ventricular EGM presented here is feasible, reproducible, and may significantly quantify changes in Phases 0-1 of the endocardial cardiac AP and ventricular repolarization induced by select antiarrhythmic medications. The current automated methods to discriminate SVTs from VTs using existing EGM models and morphologic techniques continue to result in a significant number of inappropriate shocks. A recent study<sup>42</sup> reports that 23-30% of patients are subject to inappropriate shocks. The majority of these inappropriate shocks were due to misclassification of rapidly conducted SVTs. The novel segmentation approach of this model sheds insight into the factors that predispose to ventricular arrhythmias (e.g., changes to the subendocardial AP) thus, may afford ICDs a higher sensitivity for detecting true ventricular arrhythmias.

Current ICDs are quite sophisticated but remain limited in computational power and generally consist of an 8-bit microprocessor with a 2.6 megahertz clock and 256 kilobytes of memory.<sup>43</sup> This is paltry in comparison to the laptop PC used in this study equipped with a 32-bit microprocessor with a 1.6 gigahertz clock and 1 gigabyte of memory. The type of model described here is simple enough that it can be implemented in the typical digital signal processor contained in a cardiac device such as a pacemaker or a cardioverter-defibrillator with existing technologies. Thus, using currently available implantable device technology, this model may provide a valuable technique to discriminate between arrhythmias of various origins and more importantly, may provide a quantitative means to assess cardiac ion channel function through the analysis of cardiac EGMs.

### Limitations of this Study

There are several limitations to the data presented here. First, there are limits of the method related to the level of changes one would expect

on the EGM. The isolated analog-input can accept a voltage range of  $\pm 50$  mV (the rabbit EGMs fall within this range) and apply a gain of 200. The ADC can detect a 0.004 mV change in the input signal at the smallest input range. Thus, providing a resolution of 0.004 mV on the EGM input signal. The EGM standardization procedure utilized in this study permits us to focus upon the relative change in EGM signals from baseline rather than their absolute amplitude. The ADC has a frequency resolution of 200 kilosamples/s however, the EGMs input to the ADC are presampled by the pacemaker at 250 samples/s. Thus, our frequency bandwidth is limited to at most half of the sampling frequency or 125 samples/s. This is well above the "frequency-of-interest" range used in other research on human EGM analysis algorithm development, typically 1-44 samples/s (or Hertz).<sup>44-46</sup> There is a caveat however, it has been shown that VT EGMs have minor high-frequency components<sup>28</sup> when compared to NSR beats. As described in the Methods section, we applied a 5-point moving average to the raw EGMs which in effect is equivalent to applying a low-pass filter to the raw signal. This may remove some higher frequency signals which may make our model less sensitive in detecting subtle signal changes. The EGMs obtained from ICDs implanted in humans will not require this aggressive filtering. Prototype devices that allow chronic percutaneous sampling of raw electrical signals can be considered. Third, the size-constraints of the rabbit heart may preclude the use of chronic intracardiac catheters to obtain endocardial EGMs. The application of this model to the human ICD EGM will permit analysis of the endocardial unipolar EGM. Finally, the physiologic significance of each order coefficient in our model remains to be elucidated.

### CONCLUSION

This study demonstrated that a polynomial model of the rabbit ventricular EGM is feasible, reproducible, and responds to pharmacologic interventions in a quantifiable fashion. The model presented here preserves computational simplicity to permit implementation in current, low computational power implantable devices. Ventricular EGMs may not have long-term stability.<sup>45,46,13</sup> Therefore, one could look at a change in coefficients rather than absolute value. Heuristic featuring leads to information loss, whereas sample-based featuring is more appropriate.<sup>28</sup> Hence, modeling

the system using its baseline features will minimize information loss.

The development of an EGM model may ultimately enable detailed analysis of medication effects, arrhythmias, and arrhythmic substrates by examining the changes in the model with various interventions. These data may provide a valuable technique to discriminate ventricular from SVTs and more importantly, may provide a quantitative means to assess cardiac ion channel function through the analysis of cardiac EGMs. Long-term applications of this new method may include incorporating it into cardiac devices such as pacemakers and defibrillators where the ventricular EGMs can be used to monitor physiologic changes ranging from ischemia to electrolyte disturbances and to provide a new tool to quantify the action of anti-arrhythmic medications and assess cardiac ion channel function. In addition, similar modeling techniques can be applied to EGMs from other cardiac chambers, namely the atria, to provide a more complete picture of the electrical status of the heart.

**Acknowledgment:** *This work was supported in part by an ACCF/Merck 2005-2006 Research Fellowship.*

## REFERENCES

- Bland JM, Altman DG. Statistical methods for assessing agreement between two methods of clinical measurement. *Lancet* 1986;1:307-310.
- Liu G, Iden JB, Kovithavongs K, et al. In vivo temporal and spatial distribution of depolarization and repolarization and the illusive murine T wave. *J Physiol* 2003;555.1:267-279.
- Nam GB, Burashnikov A, Antzelevitch C. Cellular mechanisms underlying the development of catecholaminergic ventricular tachycardia. *Circulation* 2005;111:2727-2733.
- Aslanidi OV, Clayton RH, Lambert JL, et al. Dynamical and cellular electrophysiological mechanisms of ECG changes during ischemia. *J Theor Biol* 2005;237(4):369-381.
- Whalley DW, Wendt DJ, Starmer CF, et al. Voltage-independent effects of extracellular K<sup>+</sup> on the Na<sup>+</sup> current and phase 0 of the action potential in isolated cardiac myocytes. *Circ Research* 1994;75(3):491-502.
- Mukhopadhyay S, Sircar P. Parametric modelling of ECG signal. *Med & Biol Eng & Comput* 1996;34:171-174.
- Dingfei G, Srinivasan N, Krishnan SM. Cardiac arrhythmia classification using autoregressive modeling. *Biomed Eng Online* 2002;1(5):1-12.
- Finelli CJ. The time-sequenced adaptive filter for analysis of cardiac arrhythmias in intraventricular electrograms. *IEEE Transactions Biomed Eng* 1996;43(8):811-819.
- DiCarlo LA, Jenkins JM, Winston SA, et al. Differentiation of ventricular tachycardia from ventricular fibrillation using intraventricular electrogram morphology. *Am J Card* 1992;70:820-822.
- Stevenson SA, Jenkins JM, DiCarlo LA. Analysis of the intraventricular electrogram for differentiation of distinct monomorphic ventricular arrhythmias. *PACE* 1997;20:2730-2738.
- Finelli CJ, DiCarlo LA, Jenkins JM, et al. Effects of increased heart rate and sympathetic tone on intraventricular electrogram morphology. *Am J Cardiol* 1991;68:1321-1328.
- Davies DW, Wainwright RJ, Tooley MA, et al. Detection of pathological tachycardia by analysis of electrogram morphology. *PACE* 1986;9:200-208.
- Throne RD, Jenkins JM, DiCarlo LA. A comparison of four new time-domain techniques for discriminating monomorphic ventricular tachycardia from sinus rhythm using ventricular waveform morphology. *IEEE Trans Biomed Eng* 1991;38(6):561-570.
- Gold MR, Hsu W, Marcovecchio AF, et al. A new defibrillator discrimination algorithm utilizing electrogram morphology analysis. *PACE* 1999;22(Part II):179-182.
- Lux RL. Karhunen-Loeve representation of ECG data. *J Electrocardiol* 1992;25(Suppl.):195-198.
- Laguna P, Garcia J, Roncal I, et al. Model-based estimation of cardiovascular repolarization features: Ischaemia detection and PTCA monitoring. *J Med Eng Technol* 1998;22(2):64-72.
- Garcia J, Lander P, Sornmo L, et al. Comparative study of local and Karhunen-Loeve-based ST-T indexes in recordings from human subjects with induced myocardial ischemia. *Comput Biomed Res* 1998;31(4):272-292.
- Laguna P, Moody GB, Garcia J, et al. Analysis of the ST-T complex of the electrocardiogram using the Karhunen-Loeve transform: Adaptive monitoring and alternans detection. *Med Biol Eng Comput* 1999;37(2):175-189.
- Coggins RJ, Jabri MA. A low-complexity intracardiac electrogram compression algorithm. *IEEE Trans Biomed Eng* 1999;46(1):82-91.
- Lamothe R, Stroink G. Orthogonal expansions: Their applicability to signal extraction in electrophysiological mapping data. *Med Biol Eng Comput* 1991;29(5):522-528.
- Berenfeld O, Abboud S. Simulation of cardiac activity and the ECG using a heart model with a reaction-diffusion action potential. *Med Eng Phys* 1996;18(8):615-625.
- Dhein S, Muller A, Gerwin R, et al. Comparative study on the proarrhythmic effects of some antiarrhythmic agents. *Circulation* 1993;87(2):617-630.
- Henriquez CS, Plonsey R. Simulation of propagation along a cylindrical bundle of cardiac tissue- I: Mathematical formulation. *IEEE Trans Biomed Eng* 1990;37(9):850-860.
- Spach MS, Miller WT, Geselowitz DB, et al. The discontinuous nature of propagation in normal canine cardiac muscle. Evidence for recurrent discontinuities of intracellular resistance that affect the membrane currents. *Circ Res* 1981;48:39-54.
- Joly D, Savard P, Roberge FA, et al. Simulation and experimental studies of the factors influencing the frequency spectrum of cardiac extracellular waveforms. *J Electrocard* 1990;23(2):109-125.
- Roelke M, Garan H, McGovern BA, et al. Analysis of the initiation of spontaneous monomorphic ventricular tachycardia by stored intracardiac electrograms. *JACC* 1994;23(1):117-122.
- Muzikant AL, Hsu EW, Wolf PD, et al. Region specific modeling of cardiac muscle: Comparison of simulated and experimental potentials. *Ann Biomed Eng* 2002;30(8):867-883.
- Rojo-Alvarez JL, Arenal-Maiz A, Artes-Rodriguez A. Discriminating between supraventricular and ventricular tachycardias from EGM onset analysis. *IEEE Eng Med Bio* 2002:16-26.
- Spach MS, Barr RC. Origin of epicardial ST-T wave potentials in the intact dog. *Circ Research* 1976;39(4):475-487.

30. Spach MS, Barr RC. Analysis of ventricular activation and repolarization from intramural and epicardial potential distributions for ectopic beats in the intact dog. *Circ Research* 1975;37:830-843.
31. Harumi K, Burgess MJ, Abildskov JA. A theoretic model of the T wave. *Circ* 1966;XXXIV:657-668.
32. Burgess MJ, Harumi K, Abildskov JA. Application of a theoretic T-wave model to experimentally induced T-wave abnormalities. *Circ* 1966;XXXIV:669-678.
33. Gima K, Rudy Y. Ionic current basis of electrocardiographic waveforms. A model study. *Circ Res* 2002;90:889-896.
34. London B. Cardiac arrhythmias: From transgenic mice to men. *J Cardiovasc Electrophysiol* 2001;12(9):1089-1091.
35. Janse MJ, Kleber AG, Capucci A, et al. Electrophysiological basis for arrhythmias caused by acute ischemia. *J Mol Cell Cardiol* 1986;18:339-355.
36. Franz MR. Method and theory of monophasic action potential recording. *Prog Cardiovas Dis* 1991;33(6):347-368.
37. Franz MR. Current status of monophasic action potential recording: Theories, measurements and interpretations. *Cardiovasc Res* 1999;41:25-40.
38. Josephson ME, Harken AH, Horowitz LN. Endocardial excision: A new surgical technique for the treatment of recurrent ventricular tachycardia. *Circulation* 1979;60(7):1430-1439.
39. Josephson ME, Horowitz LN, Spielman SR, et al. Role of catheter mapping in the preoperative evaluation of ventricular tachycardia. *Am J Cardiol* 1982;49:207-220.
40. Sager PT, Batsford WP. Ventricular arrhythmias: Medical therapy, device treatment, and indications for electrophysiologic study. *Cardiology Clinics* 1988;6(1):37-47.
41. Ferrier GR, Guyette CM. Ventricular tachycardia in an isolated guinea pig ventricular free wall model of ischemia and reperfusion. *J Cardiovasc Pharmacol* 1991;17(2):228-238.
42. Sweeney MO, Wathen MS, Volosin K, et al. Appropriate and inappropriate ventricular therapies, quality of life, and mortality among primary and secondary prevention implantable cardioverter defibrillator patients: Results from the pacing fast VT reduces shock therapies (PainFREE Rx II) Trial. *Circulation* 2005;111:2898-2905.
43. Graves-Calhoun A. Personal Communication. Medtronic Inc., Minneapolis, MN, 2005.
44. Paul VE, O'Nunain S, Malik M, et al. Temporal electrogram analysis: Algorithm development. *PACE* 1990;13(Part II):1943-1947.
45. Hook BG, Marchlinski FE. Value of ventricular electrogram recording in the diagnosis of arrhythmias precipitating electrical device shock therapy. *JACC* 1991;17(4):985-990.
46. Barold HS, Newby KH, Tomassoni G, et al. Prospective evaluation of new and old criteria to discriminate between supraventricular and ventricular tachycardia in implantable defibrillators. *PACE* 1998;21:1347-1355.